

A-7-3

Effect of Ultra-thin Al₂O₃ Insertion on Fermi-level Pinning at Metal/Ge Interface

Tomonori Nishimura, Koji Kita and Akira Toriumi

 Department of Materials Engineering, School of Engineering, The University of Tokyo
 7-3-1 Hongo, Bunkyo, Tokyo 113-8656, Japan

Phone: +81-3-5841-7161 E-mail: nishimura@adam.t.u-tokyo.ac.jp

1. Introduction

Ge is very attractive semiconductor to design advanced CMOS beyond the scaling limit of Si. However, in the Ge CMOS generation the contact and diffusion layer resistances will be more dominant than the channel one. To overcome the challenge, ultra-short channel Schottky source/drain FETs will be also a possible candidate for Ge devices. Then, a precise elucidation of metal/Ge junction characteristics is strongly required. Dimoulas et al. [1] and our group [2] independently found the strong Fermi-level pinning (FLP) close to the valence band edge of Ge. On the other hand, it is clearly shown in *C-V* characteristics that the surface potential in Ge MIS capacitors is modulated without a strong FLP at insulator/Ge interface.

This paper discusses the origin of FLP at metal/Ge junction, focusing on the change of strength and charge neutrality level (CNL) from Ge M/S to Ge MIS diodes by changing the insulator thickness.

2. Experimental

Both n- and p-type Ge (100) substrates were cleaned by using methanol, HCl, H₂O₂ + NH₄ and HF. Al₂O₃ was employed for an insulator to insert into the junction interface, because it has a wide band gap and works as the oxidation diffusion barrier. Al₂O₃ films were deposited on Ge by rf-sputtering at room temperature. The post deposition annealing (PDA) was performed in N₂ at 400 °C. The Al₂O₃ thickness was estimated by sputtering time and by grazing incident X-ray reflectivity measurement. It was confirmed with AFM that no surface roughness increase associated with sputtering and PDA was observed (rms value=0.35 nm for Ge and 0.37 nm for Al₂O₃ after PDA). The 50 nm-thick and 200 μm-diameter electrode metals were thermally evaporated on the substrates in a conventional vacuum chamber for Au and Al and evaporated by electron beam in UHV (~10⁻⁸ Pa) condition for Y and Ni.

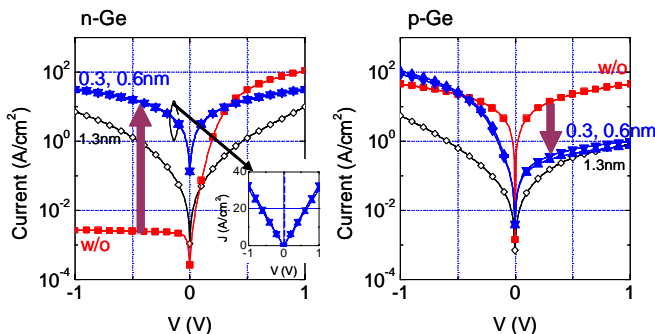


Fig. 1 *J-V* characteristics for MIS diode with thin Al₂O₃. The Al₂O₃ thickness are 1.3(◇), 0.6(▲), 0.3(▼) and 0(w/o)(■) nm.

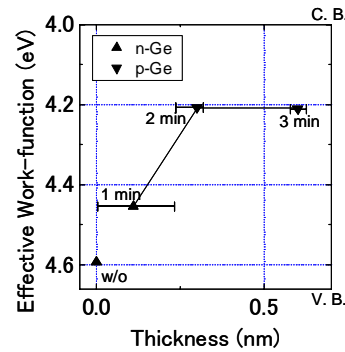


Fig. 2 W_{eff} transition of Au with increasing Al₂O₃ thickness. W_{eff} s are determined by SBHs of n-Ge(▲) and p-Ge(▼). By Al₂O₃ insertion, W_{eff} obviously shifted from valence band edge to conduction band side.

3. Results

J-V characteristics of Au/ultra-thin Al₂O₃/Ge were measured in the range of ±1 V, as shown in **Fig. 1**. Both metal/Ge junctions on n- and p-Ge show Schottky and ohmic characteristics, respectively. However, it is noted that the rectification characteristics are obviously changed from Schottky to ohmic on n-Ge and ohmic to Schottky on p-Ge by inserting 0.3 or 0.6 nm (sputtering time; 2 or 3 min.) ultra-thin Al₂O₃. In the case of 1.3 nm Al₂O₃ film insertion (sputtering time; 5 min), the conductance is significantly reduced.

Schottky barrier height (SBH) was evaluated from the conventional *J-V* method with following equations (for n-type semiconductor),

$$J = J_s (e^{\frac{qV}{kT}} - 1), \quad J_s = A^* T^2 e^{-\frac{q\phi_b}{kT}}$$

, where J_s is the saturation current density is evaluated by linear extrapolation from reverse bias value at $V=0$, and A^* is the Richardson constant (about 140 for n-Ge, 48 A/cm²/K² for p-Ge [3]). Effective work-functions (W_{eff}) are defined as $q\chi_{\text{Ge}}$ (electron affinity of Ge) + $q\phi_{\text{bn}}$ (SBH for n-Ge) or $q\chi_{\text{Ge}} + E_g - q\phi_{\text{bp}}$ (SBH for p-Ge). The relationship between W_{eff} and the interface layer thickness are plotted in **Fig. 2**. The W_{eff} of Au certainly shifts by 0.38 eV from valence band edge to conduction band side with increasing Al₂O₃ thickness.

The metal work-function dependence of W_{eff} was evaluated for four kinds metal/Ge junctions with 0.6 nm-thick Al₂O₃. Note that **Fig. 3** shows almost the same W_{eff} values (~4.2 eV) for metals with the work-function ranging from 3 to 5 eV. This fact means that Al₂O₃ insertion brings about another strong FLP with a different CNL from that of M/S junctions. **Figure 4** clearly describes a distinct shift of the CNL between metal/Ge and metal/ultra-thin Al₂O₃/Ge diodes.

We confirmed thick Al₂O₃ (~5 nm)/Ge MIS capacitor characteristics, as shown in **Fig. 5**. Au and Al were made on a same substrate. The *C-V* curve indicates that the sur-

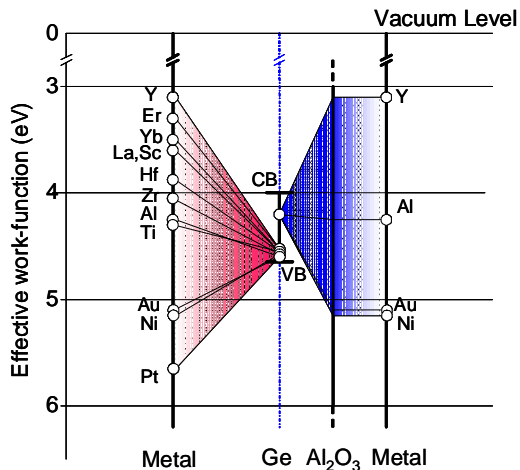


Fig. 3 W_{eff} transition from metal to metal/Ge and metal to metal /thin $\text{Al}_2\text{O}_3/\text{Ge}$. M/S junction data were re-plots of the previous one [2].

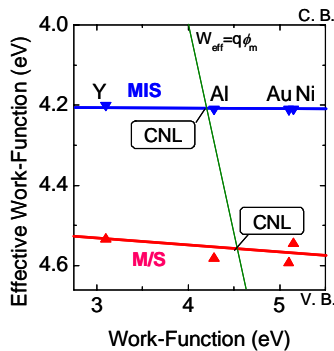


Fig. 4 Metal work-function dependence of W_{eff} for metal/Ge (\blacktriangle) and metal/ $\text{Al}_2\text{O}_3(0.6\text{nm})/\text{Ge}$ (\blacktriangledown). From the $W_{\text{eff}} = q\phi_m$ line, CNL of M/S and that of MIS are obtained to be 4.58 and 4.21 eV. The CNL shift is 0.37 eV.

face potential at $\text{Al}_2\text{O}_3/\text{Ge}$ interface is varied by gate bias, and that V_{FB} difference between Al and Au MIS capacitors is about 0.8 eV, which is in agreement with the vacuum work function difference. This means that the strong FLP observed at metal/Ge junctions is substantially unpinned by inserting thick Al_2O_3 between metal and Ge.

4. Discussion

We proposed the intrinsic metal-induced gap states (MIGS) model for the metal/Ge strong FLP [2]. In the MIGS model, FLP is explained by tailing of metal wave function into the Ge gap states from metal side. Then, the FLP strength is described by the penetration length of the metal wave function and the virtual gap states of Ge, while CNL is determined by the branch point of bulk Ge [4]. It is, however, difficult to explain FLP results in MIS diodes with ultra-thin Al_2O_3 film by the same MIGS model. It is generally recognized that the penetration length of metal wave function is short enough (\sim several \AA [4]) to smear out the MIGS effect. On the other hand, MIS capacitors with thick Al_2O_3 have shown unpinned character in terms of the V_{FB} shift. Therefore, the FLP at MIS diodes with ultra-thin Al_2O_3 must be attributed to the interaction between metal and Ge. Our speculative view is as follows. The results seem to indicate that with the insertion of Al_2O_3 film the initially existing MIGS disappears and another new FLP origin appears. In the case of ultra-thin Al_2O_3 films, the metal wave function will be able to interact with Ge dangling bonds in terms of “metal-Ge bonding” rather than

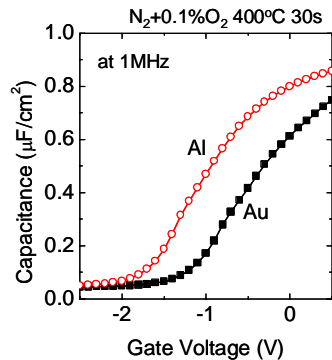


Fig. 5 C-V characteristics for metal / thick Al_2O_3 ($\sim 5\text{nm}$) /n-Ge MIS device. Surface potential were varied. Furthermore, the V_{fb} difference caused by metal work function can be seen. Fermi level at $\text{Al}_2\text{O}_3/\text{Ge}$ interface is not pinned.

M/S	MIS (ultra-thin Al_2O_3)	MIS (thick Al_2O_3)
CNL Bulk Ge	Metal-Ge interaction	Al_2O_3
Density of interface states Large	Large	Small
FLP > strong FLP at CNL-1	> strong FLP at CNL-2	> unpinned

Table 1 Schematic diagrams for FLP at Ge junction. The table shows FLP description, CNL (FLP level) and effective density of interface states (FLP strength), respectively.

“the wave function penetration”. Through the energy level induced by the dangling bond will serve as a new CNL within the energy gap, which is closely related to the disorder-induced gap states (DIGS) [5]. These descriptions are schematically summarized in **Table 1**.

5. Conclusion

By inserting ultra-thin Al_2O_3 film into metal/Ge junction interface, FLP strength and CNL are drastically varied. This fact suggests that the origin of FLP at Ge junction system changes from the bulk Ge MIGS to the interface DIGS with the change from M/S to MIS structures.

Acknowledgement

This work was partly supported by a Grant-in-Aid for Scientific Research from the Ministry of Education, Culture, Sports, Science and Technology in Japan.

Reference

- [1] A. Dimoulas *et. al*, Appl. Phys. Lett. **89**, 252110 (2006).
- [2] T. Nishimura *et. al*, Ext. Abs. SSDM, p. 400 (2006).
- [3] S. M. Sze; “The Physics of Semiconductor Devices” John Wiley & Sons Inc., p. 257 (1981).
- [4] J. Tersoff, Phys. Rev. Lett. **52**, 465 (1984).
- [5] H. Hasegawa and H. Ohno, J. Vac. Sci. Technol. B **4**, 1130 (1986).